Commun. Comput. Phys.
doi: 10.4208/cicp.250313.281013a

Vol. **15**, No. 5, pp. 1431-1460
May 2014

An Unpreconditioned Boundary-Integral for Iterative Solution of Scattering Problems with Non-Constant Leontovitch Impedance Boundary Conditions

D. Levadoux[1], F. Millot[2] and S. Pernet[3,*]

[1] *ONERA, French Aerospace Lab, Chemin de la humière 91761 Palaiseau, France.*
[2] *CERFACS 42 avenue G. Coriolis 31057 Toulouse, France.*
[3] *ONERA, French Aerospace Lab, 2 Avenue Édouard Belin, 31000 Toulouse, France.*

Received 25 March 2013; Accepted (in revised version) 28 October 2013

Communicated by Jan S. Hesthaven

Available online 5 March 2014

Abstract. This paper concerns the electromagnetic scattering by arbitrary shaped three dimensional imperfectly conducting objects modeled with non-constant Leontovitch impedance boundary condition. It has two objectives. Firstly, the intrinsically well-conditioned integral equation (noted GCSIE) proposed in [30] is described focusing on its discretization. Secondly, we highlight the potential of this method by comparison with two other methods, the first being a two currents formulation in which the impedance condition is implicitly imposed and whose the convergence is quasi-optimal for Lipschitz polyhedron, the second being a CFIE-like formulation [14]. In particular, we prove that the new approach is less costly in term of CPU time and gives a more accurate solution than that obtained from the CFIE formulation. Finally, as expected, It is demonstrated that no preconditioner is needed for this formulation.

AMS subject classifications: 65R20, 15A12, 65N38, 65F10, 65Z05

Key words: Integral equation, boundary element method, impedance boundary equation, preconditioner, GMRES, fast multipole method.

1 Introduction

The boundary integral methods (BIM) are commonly used for solving scattering problems of arbitrarily shaped three-dimensional obstacles and also for antenna design. Their

*Corresponding author. *Email addresses:* `David.Levadoux@onera.fr` (D. Levadoux), `millot@cerfacs.fr` (F. Millot), `Sebastien.Pernet@onera.fr` (S. Pernet)

popularity is due to a combination of many factors. Firstly, the solutions of BIM fulfill causality and radiation conditions automatically. Secondly, it is only necessary to discretize the boundaries of the computational domain and the simulation requires a smaller number of unknowns than finite element methods or finite difference methods. One of the main drawbacks of using a BIM is that after discretization it results in a dense system of linear equations. If a large number of unknowns is involved, the only possibility is to use iterative solvers coupled with a fast matrix-vector multiplication. However, with such a tool various situations can be analyzed, for instance conductor obstacles, dielectric homogeneous obstacles and also imperfectly conductor materials. We focus our attention on imperfectly conducting materials. This type of materials is generally taken into account by imposing an impedance boundary condition like the Leontovitch condition [22] on the surface of the object. Such situations occur in radar applications: objects are often partially coated by a thin dielectric layer to reduce the radar cross section of scattering waves. Another domain of application of such boundary conditions is their use as an absorbing boundary condition to limit the computational domain. Several boundary integral formulations can be derived to solve such impedance problems. Most representatives are formulations using one current as the unknowns proposed in [1,5,14,26,29], the system of integral equations based on the minimization of a quadratic functional in [13] and a formulation keeping the two currents as unknowns obtained, in particular, in [21]. The equivalent currents are discretized by a boundary-element method over a triangular mesh on the surface. Finally, we obtain a dense linear system. When the characteristic size of the obstacle is about six times the wavelength, the solutions can be computed by direct methods with high performance parallel codes. However, if the size of the obstacle increases, the solutions can only be obtained by means of some iterative methods coupled with the multilevel fast multipole method (noted MFMM). The convergence of the iterative methods is directly linked to the choice of the integral formulation. So, the main difficulty is to choose the best boundary equation in the sense that this equation gives rise to a well-conditioned linear system and also in the sense that the solutions must be accurate. An algebraic preconditioner [11] is generally used to improve the convergence of the iterative solver. Unfortunately, this kind of approach loses its effectiveness when the frequency increases or the meshes become denser with respect to the wavelength.

Recently, another alternative is emerged. It consists of constructing new integral equations that give rise to intrinsically well-conditioned linear systems. The genesis of these techniques are the work of D. Levadoux at ONERA. Indeed, in his thesis [23–25], he initiated a new integral formalism known as GCSIE (Generalized Combined Source Integral Equation) in which he has combined pseudo-differential mathematical analysis and physical characteristics of waves to obtain integral equations well-adapted to an iterative solution. These works have led to the emergence of a general formalism of construction which has been used, with success, for many problems in acoustics and in electromagnetism. The new formalism depends on the choice of an operator. This one aims to be a good approximation of the admittance in the perfectly metallic case. Several propositions have already made to achieve this goal [3,4,6,7,18,31]. The numerical results are

impressive in term of reducing of the number of iterations and the CPU time. We showed in [16,30] that the impedance problems can be understood by the GCSIE formalism. This always depends on knowing the optimal regularizing operator. In this paper, we first want to focus on the numerical aspects of this formalism. Secondly, a comparison with the commonly used classical BIM formulations is presented. More precisely, we focus on the CPU time and the memory storage needed to obtain the solution as well as the accuracy.

The paper is divided as follows. In Section 2, we present the scattering problem to be solved. In particular, we first briefly introduce the new approach used to construct the boundary integral equations in electromagnetism. We revise the classical integral equations for impedance obstacles in Section 3. The discretization is presented in Section 4. The final section is devoted to numerical results.

2 Intrinsically well-conditioned integral equation

This section is divided into two parts. The first presents the scattering problem. The second explains how to derive a well-conditioned integral equation in the context of the Leontovitch boundary condition.

2.1 The scattering problem

Let Ω^- be a Lipschitz polyhedron with a boundary Γ which is assumed to be simply connected. The open complement of Ω^- in $\mathbb{R}^3$ is Ω^+. The vector $\mathbf{n}$ denotes the unit normal to Γ pointing into the exterior domain Ω^+ of Ω^-. The problem is to find the electromagnetic fields $\mathbf{E}$ and $\mathbf{H}$ which give the solution to the Maxwell system

$$\begin{cases} \mathrm{curl}\,\mathbf{E} - ikZ_0\mathbf{H} = 0 & \text{in } \Omega^+, \\ \mathrm{curl}\,\mathbf{H} + ikZ_0^{-1}\mathbf{E} = 0 & \text{in } \Omega^+, \end{cases} \tag{2.1}$$

completed with both the Silver-Müller radiation condition at infinity

$$\lim_{|x|\to\infty} |x| \left(\mathbf{E}(x) + Z_0 \frac{x}{|x|} \times \mathbf{H}(x) \right) = 0 \tag{2.2}$$

and the boundary conditions on the surface Γ

$$\mathbf{n} \times (\mathbf{E}_{|\Gamma} \times \mathbf{n}) - Z_0 \eta (\mathbf{n} \times \mathbf{H}_{|\Gamma}) = \mathbf{g}, \tag{2.3}$$

where $k > 0$ is the wavenumber, Z_0 is the intrinsic impedance of the vacuum and $\eta(x)$ is an impedance function. The variations of $\eta(x)$ allows us to take into account the presence of different materials on the surface Γ of the obstacle (see Fig. 1).

We have the following existence and the uniqueness results (see [19] for a proof and [28] for details on this kind of techniques):

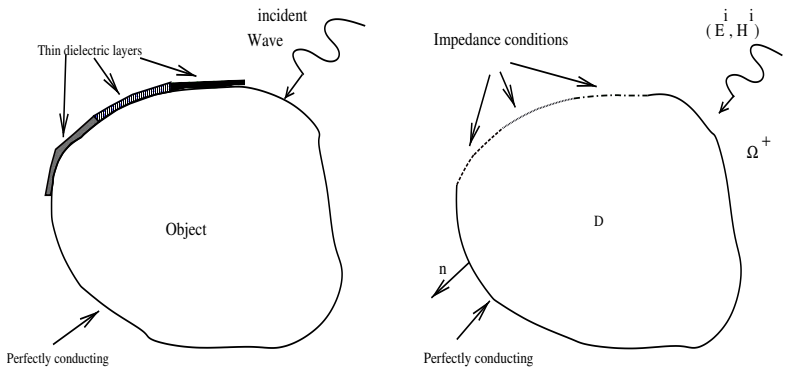

Figure 1: Exact problem on left and approximate physical model on right to be solved.

Theorem 2.1. *We assume that:*

- Ω^- *is a connected Lipschitz polyhedral domain;*
- $g \in \mathbf{L}^2_T(\Gamma)$;
- $\eta \in L^\infty(\Gamma)$ *and is assumed to be a strictly-positive real-valued function.*

Then the exterior mixed boundary value problem (2.1), (2.2), (2.3) *has a unique solution which belongs to the space* $X_{loc}(\Omega^+,\Gamma) := \{\mathbf{u} \in \mathbf{H}_{loc}(curl,\Omega^+) : \mathbf{n}\times\mathbf{u}_{|\Gamma} \in \mathbf{L}^2_T(\Gamma)\}$, *where* $\mathbf{L}^2_T(\Gamma) = \{\mathbf{u} \in [L^2(\Gamma)]^3 : \mathbf{u}\cdot\mathbf{n} = 0\}$.

Remark 2.1. In what follows, we assume that the assumptions of the Theorem 2.1 hold. In particular, the impedance function $\eta(x)$ is assumed to be piecewise constant. For simplicity, we only consider in following, the scattering by an incident plane wave $(\mathbf{E}^{\text{inc}},\mathbf{H}^{\text{inc}})$ leading to $\mathbf{g} = -\mathbf{n}\times(\mathbf{E}^{\text{inc}}_{|\Gamma}\times\mathbf{n}) - Z_0\eta(\mathbf{n}\times\mathbf{H}^{\text{inc}}_{|\Gamma})$.

2.2 Derivation of the intrinsically well-conditioned integral equation

2.2.1 Principle of the method

Let W be the space of all fields verifying both the Maxwell equations in Ω^+ and the Sliver-Müller condition. Moreover, we define the trace operator Γ associated to impedance boundary condition (2.3): let $w = (\mathbf{E},\mathbf{H}) \in W$ then we define $\gamma w = \mathbf{n}\times(\mathbf{E}_{|\Gamma}\times\mathbf{n}) - Z_0\eta(\mathbf{n}\times\mathbf{H}_{|\Gamma})$.

The problem we plan to solve, can be written as

$$\text{Find } w \in W \text{ such that } \gamma w = \mathbf{g}. \tag{2.4}$$

Moreover, by using the Stratton-Chu formulae (see the next part), it can be known that any field $w = (\mathbf{E},\mathbf{H}) \in W$ can be rebuilt from the knowledge of its Cauchy data $\gamma_c w = (\mathbf{n}\times\mathbf{E}_{|\Gamma},\mathbf{n}\times\mathbf{H}_{|\Gamma})$ via a Calderón potential $\mathcal{C}$ i.e., $w = \mathcal{C}(\gamma_c w)$ (see (2.10)). The main idea to

build a new class of boundary integral equations is based on some remarks. First, as the initial problem (2.4) to solve is well-posed, there exists an operator $\mathbf{Y}^{ex}$ defined by

$$\mathbf{Y}^{ex}: \gamma w \mapsto \gamma_c w. \tag{2.5}$$

We have to keep in mind that $\mathbf{Y}^{ex}$ is a boundary operator which by definition verifies the crucial relation

$$\gamma \mathcal{C} \mathbf{Y}^{ex} = \mathrm{Id}, \tag{2.6}$$

where Id is the identity operator on Γ.

Secondly, let $\mathbf{Y}$ be an approximation of $\mathbf{Y}^{ex}$. We decide to look for the solution w of the initial problem (2.4) under the form

$$w = \mathcal{C} \mathbf{Y} \tilde{\mathbf{g}}, \tag{2.7}$$

where $\tilde{\mathbf{g}}$ is a current distribution on Γ acting as a source excitation of the potential $\mathcal{C}\mathbf{Y}$. Therefore, in order to find a source $\tilde{\mathbf{g}}$ radiating the field solution of our initial problem (2.4), we have to solve the resulting source (or indirect) integral equation

$$\gamma \mathcal{C} \mathbf{Y} \tilde{\mathbf{g}} = \mathbf{g}. \tag{2.8}$$

Because of the crucial relation (2.6), if $\mathbf{Y} = \mathbf{Y}^{ex}$ the new equation (2.8) becomes trivial. Therefore, we suspect that when $\mathbf{Y}$ is a good approximation of $\mathbf{Y}^{ex}$, the resulting equation is a "small" perturbation of identity which produces after discretization a well-conditioned linear system.

In practice, the operator $\mathbf{Y}$ is constructed by using the pseudo-differential calculi with the objective to obtain an integral operator $\gamma\mathcal{C}\mathbf{Y}$ which decomposes under the form of an "Identity operator" plus "a compact operator". It is well known that this type of equation is well-adapted to an iterative solution and that if the spectral behavior of the equation is well restored to the discrete level, then the convergence rate is independent to space and frequency refinement [32, 33]. That is why this technique is attractive, compared to the classical algebraic preconditioners like SPAI (SParse Approximate Inverse) where the k and h-dependencies are not obvious to take into account. More precisely, in order to be efficient, the filling of the SPAI must be adjusted as a function to the complexity of the problem. To conclude, the GCSIE simplifies the work of the user by regularizing the pathological behavior of operations at the continuous level.

2.2.2 Formal mathematical construction of the integral equation

First, let us define some functional spaces which allow us to correctly define the trace and integral operators in the context of Lipschitz polyhedral domains [8]. The tangential trace operator γ_t is defined by:

$$\begin{array}{rccc} \gamma_t: \mathbf{H}(\mathrm{curl},\Omega) & \to & \mathbf{H}_{\times}^{-1/2}(\mathrm{div}_{\Gamma},\Gamma), \\ \mathbf{u} & \mapsto & \mathbf{n}\times\mathbf{u}, \end{array} \tag{2.9}$$

is continuous, surjective and possesses a right inverse, where

$$\mathbf{H}_{\times}^{-1/2}(\mathrm{div}_\Gamma,\Gamma)=\left\{\mathbf{v}\in\mathbf{H}_{\times}^{-1/2}(\Gamma):\mathrm{div}_\Gamma\mathbf{v}\in\mathrm{H}^{-1/2}(\Gamma)\right\},$$

where $\mathbf{H}_{\times}^{-1/2}(\Gamma)$ is the dual space of the Hilbert space $\mathbf{H}_{\times}^{1/2}(\Gamma)=\gamma_t(\mathrm{H}^1(\Omega))$ with respect to the pairing

$$\langle\gamma_t\mathbf{v},\gamma_t\mathbf{u}\rangle_{\tau,\Gamma}=\int_\Omega(\mathrm{curl}\mathbf{v}\cdot\mathbf{u}-\mathbf{v}\cdot\mathrm{curl}\mathbf{u})dx$$

and div_Γ is the adjoint operator of $-\nabla_\Gamma$. Moreover, we define the Hilbert space $\mathbf{H}_{\perp}^{1/2}(\Gamma)=\mathbf{n}\times\gamma_t(\mathrm{H}^1(\Omega))$ and $\mathbf{H}_{\perp}^{-1/2}(\Gamma)$ its dual. Finally, $\mathbf{H}_{\times}^{-1/2}(\mathrm{curl}_\Gamma,\Gamma)=\{\mathbf{v}\in\mathbf{H}_{\perp}^{-1/2}(\Gamma):\mathrm{curl}_\Gamma\mathbf{v}\in\mathrm{H}^{-1/2}(\Gamma)\}$ is the dual space $\mathbf{H}_{\times}^{-1/2}(\mathrm{div}_\Gamma,\Gamma)$ where curl_Γ is a surface operator defined as the adjoint of the operator $\mathbf{n}\times\nabla_\Gamma$.

The derivation of an integral equation is based on the Stratton-Chu formulae [8,15,28]. Defining the currents $\mathbf{J}(x)=\mathbf{n}\times\mathbf{H}_{|\Gamma}(x)$ and $\mathbf{M}(x)=-\mathbf{n}\times\mathbf{E}_{|\Gamma}(x)$, we have

$$\mathbf{E}(x)=\mathbf{E}^{\mathrm{inc}}(x)+iZ_0\tilde{\mathrm{T}}\mathbf{J}(x)+\tilde{\mathrm{K}}\mathbf{M}(x),\qquad x\in\Omega^+,\tag{2.10a}$$

$$\mathbf{H}(x)=\mathbf{H}^{\mathrm{inc}}(x)-\tilde{\mathrm{K}}\mathbf{J}(x)+iZ_0^{-1}\tilde{\mathrm{T}}\mathbf{M}(x),\quad x\in\Omega^+,\tag{2.10b}$$

where the potentials $\tilde{T}$ and $\tilde{K}$ are defined by

$$\begin{aligned}\bullet\ \tilde{\mathrm{T}}:\mathbf{H}_{\times}^{-1/2}(\mathrm{div}_\Gamma,\Gamma)&\to\mathbf{H}_{\mathrm{loc}}(\mathrm{curl}^2,\Omega^+\cup\Omega^-)\cap\mathbf{H}_{\mathrm{loc}}(\mathrm{div}0,\Omega^+\cup\Omega^-),\\ \mathbf{J}&\mapsto\tilde{\mathrm{T}}\mathbf{J}(x)=k\int_\Gamma G(x,y)\mathbf{J}(y)d\Gamma(y)\\ &\qquad+\frac{1}{k}\int_\Gamma\vec{\nabla}_xG(x,y)\mathrm{div}_\Gamma\mathbf{J}(y)d\Gamma(y),\end{aligned}\tag{2.11}$$

$$\begin{aligned}\bullet\ \tilde{\mathrm{K}}:\mathbf{H}_{\times}^{-1/2}(\mathrm{div}_\Gamma,\Gamma)&\to\mathbf{H}_{\mathrm{loc}}(\mathrm{curl}^2,\Omega^+\cup\Omega^-)\cap\mathbf{H}_{\mathrm{loc}}(\mathrm{div}0,\Omega^+\cup\Omega^-),\\ \mathbf{J}&\mapsto\tilde{\mathrm{K}}\mathbf{J}(x)=\int_\Gamma\vec{\nabla}_yG(x,y)\times\mathbf{J}(y)d\Gamma(y),\end{aligned}\tag{2.12}$$

and $G(x,y)$ is the fundamental solution for the radiating solution of the 3-D Helmholtz equation

$$G(x,y)=\frac{\exp(ik|x-y|)}{4\pi|x-y|}\tag{2.13}$$

with $\mathbf{H}_{\mathrm{loc}}(\mathcal{P},\mathcal{X}):=\{\mathbf{u}\in\mathbf{L}^2_{\mathrm{loc}}(\mathcal{X}):\mathcal{P}\mathbf{u}\in\mathbf{L}^2_{\mathrm{loc}}(\mathcal{X})\}$ and $\mathbf{H}_{\mathrm{loc}}(\mathcal{P}0,\mathcal{X}):=\{\mathbf{u}\in\mathbf{H}_{\mathrm{loc}}(\mathcal{P},\mathcal{X}):\mathcal{P}\mathbf{u}=0\}$.

Now, recall the so-called trace formulae [8,28]:

$$\mathbf{n}\times(\mathbf{E}_{|\Gamma}\times\mathbf{n})(x)=iZ_0\mathrm{T}\mathbf{J}(x)+\mathrm{K}\mathbf{M}(x)+\frac{1}{2}\mathbf{n}\times\mathbf{M}(x),\tag{2.14a}$$

$$\mathbf{n}\times(\mathbf{H}_{|\Gamma}\times\mathbf{n})(x)=-\mathrm{K}\mathbf{J}(x)-\frac{1}{2}\mathbf{n}\times\mathbf{J}(x)+iZ_0^{-1}\mathrm{T}\mathbf{M}(x),\tag{2.14b}$$

where T and K are defined by

$$\begin{array}{rcl} \mathrm{T}:\mathbf{H}_{\times}^{-1/2}(\mathrm{div}_{\Gamma},\Gamma) & \to & \mathbf{H}_{\times}^{-1/2}(\mathrm{curl}_{\Gamma},\Gamma), \\ \mathbf{J} & \mapsto & \{\gamma_t(\tilde{\mathrm{T}}\mathbf{J})\times\mathbf{n}\}_{\Gamma}, \end{array} \tag{2.15}$$

$$\begin{array}{rcl} \mathrm{K}:\mathbf{H}_{\times}^{-1/2}(\mathrm{div}_{\Gamma},\Gamma) & \to & \mathbf{H}_{\times}^{-1/2}(\mathrm{curl}_{\Gamma},\Gamma), \\ \mathbf{J} & \mapsto & \{\gamma_t(\tilde{\mathrm{K}}\mathbf{J})\times\mathbf{n}\}_{\Gamma}, \end{array} \tag{2.16}$$

where $\{\gamma_t A\times\mathbf{n}\}=(\mathbf{n}^+\times(A\times\mathbf{n}^+)+\mathbf{n}^-\times(A\times\mathbf{n}^-))/2$.

The existence and the uniqueness of the solution of problem (2.1), (2.2), (2.3) (see Theorem 2.1) induce the existence of the operator $\mathbf{Y}^{ex}=(\mathbf{Y}_M^{ex},\mathbf{Y}_J^{ex})$ such that $\mathbf{M}=\mathbf{Y}_M^{ex}\mathbf{g}$ and $\mathbf{J}=\mathbf{Y}_J^{ex}\mathbf{g}$. Consequently, the representation formulae can be written in this form:

$$\mathbf{E}(x)=iZ_0\tilde{\mathrm{T}}\circ\mathbf{Y}_J^{ex}\mathbf{g}(x)+\tilde{\mathrm{K}}\circ\mathbf{Y}_M^{ex}\mathbf{g}(x), \qquad x\in\Omega^+, \tag{2.17a}$$

$$\mathbf{H}(x)=-\tilde{\mathrm{K}}\circ\mathbf{Y}_J^{ex}\mathbf{g}(x)+iZ_0^{-1}\tilde{\mathrm{T}}\circ\mathbf{Y}_M^{ex}\mathbf{g}(x), \quad x\in\Omega^+. \tag{2.17b}$$

Using (2.3) and (2.14), we obtain the fundamental identity:

$$\mathscr{Z}^{ex}\mathbf{g}=\left(\frac{1}{2}\mathrm{Id}+\mathrm{K}\circ\mathbf{Y}_M^{ex}+iZ_0\mathrm{T}\circ\mathbf{Y}_J^{ex}+\eta Z_0\mathbf{n}\times\mathrm{K}\circ\mathbf{Y}_J^{ex}-i\eta\mathbf{n}\times\mathrm{T}\circ\mathbf{Y}_M^{ex}\right)\mathbf{g}=\mathbf{g}. \tag{2.18}$$

The operator $\mathbf{Y}^{ex}$ is generally unknown in practice and we now assume that we have an approximation $\mathbf{Y}=(\mathbf{Y}_M,\mathbf{Y}_J)$ of $\mathbf{Y}^{ex}$. So, we can parameterize the electromagnetic field solution of our problem by

$$\mathbf{E}(x)=iZ_0\tilde{\mathrm{T}}\circ\mathbf{Y}_J\tilde{\mathbf{g}}(x)+\tilde{\mathrm{K}}\circ\mathbf{Y}_M\tilde{\mathbf{g}}(x), \qquad x\in\Omega^+, \tag{2.19a}$$

$$\mathbf{H}(x)=-\tilde{\mathrm{K}}\circ\mathbf{Y}_J\tilde{\mathbf{g}}(x)+iZ_0^{-1}\tilde{\mathrm{T}}\circ\mathbf{Y}_M\tilde{\mathbf{g}}(x), \quad x\in\Omega^+, \tag{2.19b}$$

where $\tilde{\mathbf{g}}$ is a tangential vector field of Γ solution of the integral equation:

$$\mathscr{Z}\tilde{\mathbf{g}}=\left(\frac{1}{2}\mathrm{Id}+\mathrm{K}\circ\mathbf{Y}_M+iZ_0\mathrm{T}\circ\mathbf{Y}_J+\eta Z_0\mathbf{n}\times\mathrm{K}\circ\mathbf{Y}_J-i\eta\mathbf{n}\times\mathrm{T}\circ\mathbf{Y}_M\right)\tilde{\mathbf{g}}=\mathbf{g}. \tag{2.20}$$

These equations lead us to make some important comments:

- The electromagnetic field defined in (2.19) is the solution of our problem if the integral equation (2.20) is well-posed. This result is true even if $\mathbf{Y}$ is a bad approximation of the exact operator $\mathbf{Y}^{ex}$.
- If $\mathbf{Y}$ is sufficiently close to $\mathbf{Y}^{ex}$ then we expect that the approximation of the integral operator $\mathscr{Z}$ leads to a well-conditioned system.
- The unknown $\tilde{\mathbf{g}}$ of (2.20) is not a physical current. That's why this equation is called in following the GCSIE equation for Generalized Combined Source Integral Equation.

2.2.3 Convenient form of the regularized operator Y

The main point in the previous formal construction is to have a "good" approximation $\mathbf{Y}$ of the operator $\mathbf{Y}^{ex}$ or to build two approximations of $(\mathbf{Y}_J^{ex},\mathbf{Y}_M^{ex})$. To do it, we first give a more tractable expression of the exact operator:

$$\mathbf{n}\times\mathbf{M}-\eta Z_0\mathbf{J}=(\mathbf{n}\times\mathbf{Y}_M^{ex}-\eta Z_0\mathbf{Y}_J^{ex})\mathbf{g}=\mathbf{g}\quad\text{on }\Gamma. \tag{2.21}$$

Eq. (2.21) leads to a new expression of the operator $\mathbf{Y}_M^{ex}$

$$\mathbf{Y}_M^{ex}=-\mathbf{n}\times\mathrm{Id}-\eta Z_0\mathbf{n}\times\mathbf{Y}_J^{ex}. \tag{2.22}$$

Consequently, a candidate of the approximation operator $\mathbf{Y}_M$ can be chosen as:

$$\mathbf{Y}_M=-\mathbf{n}\times\mathrm{Id}-\eta Z_0\mathbf{n}\times\mathbf{Y}_J, \tag{2.23}$$

where $\mathbf{Y}_J$ is an approximation of $\mathbf{Y}_J^{ex}$.

The next step is to propose an approximation $\mathbf{Y}_J$ of $\mathbf{Y}_J^{ex}$. For that, we introduce the so-called exact exterior admittance or Stecklov-Poincaré operator $\mathscr{Y}^{ex}$ associated to the surface Γ. Recall that this operator is defined as follows: let $(\mathbf{u},\mathbf{v})$ be the solution of the well-posed problem:

$$\begin{cases}\mathrm{curl}\,\mathbf{u}-ikZ_0\mathbf{v}=0\quad\text{in }\Omega^+,\\ \mathrm{curl}\,\mathbf{v}+ikZ_0^{-1}\mathbf{u}=0\quad\text{in }\Omega^+,\\ \mathbf{n}\times\mathbf{u}\in\mathbf{H}_\times^{-1/2}(\mathrm{div}_\Gamma,\Gamma)\text{ fixed on }\Gamma,\\ +\text{ Radiation condition at infinity.}\end{cases} \tag{2.24}$$

The operator $\mathscr{Y}^{ex}$ corresponds to the operator which from $\mathbf{n}\times\mathbf{v}$ gives $\mathbf{n}\times\mathbf{u}=-\mathscr{Y}^{ex}(\mathbf{n}\times\mathbf{v})$. In particular, the current $(\mathbf{M},\mathbf{J})$ on Γ induced by the field solution of the problem (2.1), (2.2) and (2.3) are linked by the relation:

$$\mathbf{M}=\mathscr{Y}^{ex}(\mathbf{J}). \tag{2.25}$$

By using (2.3) and (2.25), one obtains a new expression of $\mathbf{Y}_J^{ex}$:

$$\mathbf{Y}_J^{ex}=\left(\mathbf{n}\times\mathscr{Y}^{ex}-\eta Z_0\mathrm{Id}\right)^{-1}. \tag{2.26}$$

To sum up, if one possesses an approximation $\mathscr{Y}$ of the admittance $\mathscr{Y}^{ex}$, it is possible to find a candidate $\mathbf{Y}_J$ for the approximation of $\mathbf{Y}_J^{ex}$ by this way:

$$\mathbf{Y}_J=\left(\mathbf{n}\times\mathscr{Y}-\eta Z_0\mathrm{Id}\right)^{-1} \tag{2.27}$$

and

$$\mathbf{Y}_M=-\mathbf{n}\times\mathrm{Id}-\eta Z_0\mathbf{n}\times\mathbf{Y}_J. \tag{2.28}$$

Finally, the integral problem (2.20) becomes: find the density $\tilde{\mathbf{g}}$ such that

$$\begin{cases} \left(\frac{1}{2}\mathrm{Id}+\mathrm{K}\circ\mathbf{Y}_M+iZ_0\mathrm{T}\circ\mathbf{Y}_J+\eta Z_0\mathbf{n}\times\mathrm{K}\circ\mathbf{Y}_J-i\eta\mathbf{n}\times\mathrm{T}\circ\mathbf{Y}_M\right)\tilde{\mathbf{g}}=\mathbf{g}, \\ \mathbf{Y}_M=-\mathbf{n}\times\mathrm{Id}-\eta Z_0\mathbf{n}\times\mathbf{Y}_J, \\ \mathbf{Y}_J=\left(\mathbf{n}\times\mathscr{Y}-\eta Z_0\mathrm{Id}\right)^{-1}, \end{cases} \tag{2.29}$$

and one may close this system if one knows an approximation $\mathscr{Y}$ of the admittance operator. In the next part, a such approximation will be proposed.

2.2.4 High frequency approximation of $\mathscr{Y}^{ex}$

The construction of the high frequency approximation $\mathscr{Y}$ of $\mathscr{Y}^{ex}$ is based on a microlocal analysis. We will firstly consider what happens on the infinite plane P and then we will extend the result to the surface Γ.

The construction begins by noting that on an infinite plane, the trace formulae (2.14) lead to the relation:

$$\mathbf{M}=-2iZ_0\mathbf{n}\times\mathrm{T}\mathbf{J}. \tag{2.30}$$

So, the admittance operator $\mathscr{Y}_P$ associated to the plane is directly obtained by $\mathscr{Y}_P=-2iZ_0\mathbf{n}\times\mathrm{T}$. Now, consider the high frequency domain and assume that the electromagnetic phenomena are localized, one expects that the operator $\mathscr{Y}^{ex}$ acts as $\mathscr{Y}_P$ where P are the tangent planes to Γ. So, the high-frequency approximation $\mathscr{Y}$ could be taken by $\mathscr{Y}_P$. Unfortunately, this choice leads to the presence of resonance frequencies [2]. In order to avoid this problem, one has to use a localization of $\mathscr{Y}_P$. That can be done at least two different ways:

- using a direct localization of $\mathscr{Y}_P$ by using an quadratic partition of the unity [2], i.e.,

$$\mathscr{Y}=\sum_i \xi_i\mathscr{Y}_P\xi_i; \tag{2.31}$$

- using an indirect localization of $\mathscr{Y}_P$ by using the Helmholtz potentials. It is this approach that we consider here, we will give some more details of this construction.

We first rewrite $\mathscr{Y}_P$ by using the single layer potential (convolution with the fundamental solution G of the Helmholtz equation):

$$\mathscr{Y}_P=2\mathbf{n}\times T=\frac{2}{ik}\mathbf{n}\times\left(\nabla_\Gamma G\nabla_\Gamma\cdot+k^2\mathbf{G}\right), \tag{2.32}$$

where $G\varphi=\int_\Gamma G(x,y)\varphi(y)d\gamma(y)$ with φ a scalar function and $\mathbf{G}\mathbf{u}=\int_\Gamma G(x,y)\mathbf{u}(y)d\gamma(y)$ with $\mathbf{u}$ a vector field on Γ.

Next, we introduce the Helmholtz or Hodge decomposition [8] of a tangent vector field $\mathbf{u}$ (with the appropriate regularity) to a surface $\mathcal{S}$:

$$\mathbf{u}=(\mathbf{n}\times\nabla_{\mathcal{S}}\Pi_{\text{loop}}+\nabla_{\mathcal{S}}\Pi_{\text{star}})\mathbf{u}, \tag{2.33}$$

where $\Pi_{\text{loop}}\mathbf{u}$ and $\Pi_{\text{star}}\mathbf{u}$ are the classical Helmholtz potentials of $\mathbf{u}$.

By introducing (2.33) in (2.32), we immediately obtain:

$$\begin{aligned}\mathscr{Y}_P\mathbf{u} &= \frac{2}{ik}\mathbf{n}\times\left(\nabla_P G\Delta_P\Pi_{\text{star}}\mathbf{u}+k^2\mathbf{G}\mathbf{n}\times\nabla_P\Pi_{\text{loop}}\mathbf{u}+k^2\mathbf{G}\nabla_P\Pi_{\text{star}}\mathbf{u}\right)\\ &= \frac{2}{ik}\mathbf{n}\times\left(\nabla_P G(\Delta_P+k^2)\Pi_{\text{star}}\mathbf{u}+k^2\mathbf{n}\times\nabla_P G\Pi_{\text{loop}}\mathbf{u}\right).\end{aligned} \tag{2.34}$$

Finally, we introduce the square-root representation of the single layer potential associated to the infinite plane P:

$$G\varphi = \frac{1}{2i}\left(\sqrt{k^2+\Delta_P}\right)^{-1}\varphi = \frac{1}{2i}\mathscr{F}^{-1}((k^2-\|\xi\|^2)^{-1/2})\varphi, \tag{2.35}$$

where $\mathscr{F}$ represents the Fourier transform and we obtain a new representation of the admittance operator $\mathscr{Y}_P$:

$$\mathscr{Y}_P\mathbf{u} = \frac{1}{k}\left(-\mathbf{n}\times\nabla_P(\Delta_P+k^2)^{\frac{1}{2}}\Pi_{\text{star}}\mathbf{u}+k^2\nabla_P(\Delta_P+k^2)^{-\frac{1}{2}}\Pi_{\text{loop}}\mathbf{u}\right). \tag{2.36}$$

To obtain an approximation $\mathscr{Y}$ of $\mathscr{Y}^{ex}$ on a surface Γ, one simply reads (2.36) on Γ by changing the differential operators defined on P by those defined on Γ and we obtain:

$$\mathscr{Y}\mathbf{u} = \frac{1}{k}\left(-\mathbf{n}\times\nabla_\Gamma(\Delta_\Gamma+k^2)^{\frac{1}{2}}\Pi_{\text{star}}\mathbf{u}+k^2\nabla_\Gamma(\Delta_\Gamma+k^2)^{-\frac{1}{2}}\Pi_{\text{loop}}\mathbf{u}\right), \tag{2.37}$$

where Δ_Γ is the Laplace-Beltrami operator and $\mathbf{u}$ is a vector field tangent to Γ.

Finally, as for the direct approach, a localization process is needed to avoid the spurious modes. This task is achieved by simply changing in (2.37) the wavenumber k into $k_\varepsilon = k+i\varepsilon$ where $i\varepsilon$ is a small imaginary part. For simplicity, we again note $\mathscr{Y}$ this new operator and $\mathbf{Y}_J$ the associated operator.

The operator $\mathscr{Y}$ as defined in (2.37) can not be used under this form in practice. Therefore, a more appropriate form is obtained by considering a Padé approximation of the square-root operator. First, let us recall that on a compact Riemann manifold, the spectrum of $-\Delta_\Gamma$ is of the form $0\le\lambda_1^2\le\lambda_2^2\le\cdots\le\lambda_n^2\le\cdots\le+\infty$. In this case the operator $(\Delta_\Gamma+k_\varepsilon^2)^{1/2}$ can be defined by

$$(\Delta_\Gamma+k_\varepsilon^2)^{\frac{1}{2}}\varphi = \sum_{p\ge1}\alpha_p(k_\varepsilon^2-\lambda_p^2)^{\frac{1}{2}}\psi_p, \tag{2.38}$$

where ψ_p are the eigenfunctions associated to λ_p and $\varphi=\sum_{p\ge0}\alpha_p\psi_p$. Consequently, if one works with the principal branch of the complex square root, then the complex number $k_\varepsilon^2-\lambda_p^2$ is more and more close to the branch cut when p increases. This implies a slow convergence of the Padé approximation and a significant cost to accurately synthesize this operator. In order to avoid this problem, we have chosen a Padé approximation

with a rotation of branch. This approximation proposed by [27] and used by Darbas-Antoine [18], is written:

$$\left(1+\frac{\Delta_\Gamma}{k_\varepsilon^2}\right)^{1/2}_{p,\theta} \equiv A_0(\theta)+\sum_{j=1}^{p} A_j(\theta)\frac{\Delta_\Gamma}{k_\varepsilon^2}\left(1+B_j(\theta)\frac{\Delta_\Gamma}{k_\varepsilon^2}\right)^{-1}. \tag{2.39}$$

We say that $(1+\Delta_\Gamma/k_\varepsilon^2)^{1/2}_{p,\theta}$ is the Padé approximation of order p and angle of rotation of branch θ of $(1+\Delta_\Gamma/k_\varepsilon^2)^{1/2}$. In order to obtain the new branch-cut, a rotation of angle θ of $\mathbb{R}_-$ is made. In practice, we use the value $\theta=\pi/3$, which corresponds to the optimal value which has been determined in the context of the On Surface Radiation Conditions for a spherical geometry [17].

Let us now come back to the approximation $\mathbf{Y}_J$ defined in (2.27). We assume that the impedance operator η is constant in order to derive the approximation operator but this choice will prove to be a good candidate in the context of a non-constant impedance. So, by using the Helmholtz decomposition, we get:

$$\begin{gathered}
\mathbf{J}=\mathbf{Y}_J g=(\mathbf{n}\times\mathscr{Y}-\eta Z_0\mathrm{Id})^{-1}\mathbf{g}\Rightarrow(\mathbf{n}\times\mathscr{Y}-\eta Z_0\mathrm{Id})\mathbf{J}=\mathbf{g}\\
\Downarrow \text{ (Helmholtz decomposition)}\\
\nabla_\Gamma\left[\frac{1}{k}\left(1+\frac{\Delta_\Gamma}{k_\varepsilon^2}\right)^{1/2}_{p,\theta}-\eta Z_0\right]\Pi_{\mathrm{star}}\mathbf{J}+\mathbf{n}\times\nabla_\Gamma\left[k\left(\left(1+\frac{\Delta_\Gamma}{k_\varepsilon^2}\right)^{1/2}\right)^{-1}_{p,\theta}-\eta Z_0\right]\Pi_{\mathrm{loop}}\mathbf{J}=\mathbf{g}.
\end{gathered} \tag{2.40}$$

This gives us the following two equations:

$$\left[\frac{1}{k}\left(1+\frac{\Delta_\Gamma}{k_\varepsilon^2}\right)^{1/2}_{p,\theta}-\eta Z_0\right]\Pi_{\mathrm{star}}\mathbf{J}=\Pi_{\mathrm{star}}\mathbf{g}, \tag{2.41a}$$

$$\left[k-\eta Z_0\left(1+\frac{\Delta_\Gamma}{k_\varepsilon^2}\right)^{1/2}_{p,\theta}\right]\Pi_{\mathrm{loop}}\mathbf{J}=\left(1+\frac{\Delta_\Gamma}{k_\varepsilon^2}\right)^{1/2}_{p,\theta}\Pi_{\mathrm{loop}}\mathbf{g}. \tag{2.41b}$$

Finally, the operator $\mathbf{Y}=(\mathbf{Y}_J,\mathbf{Y}_M)$ is defined by:

$$\begin{aligned}
\mathbf{Y}_J=&\nabla_\Gamma\left[\frac{1}{k}\left(1+\frac{\Delta_\Gamma}{k_\varepsilon^2}\right)^{1/2}_{p,\theta}-\eta Z_0\right]^{-1}\Pi_{\mathrm{star}}\cdot\\
&+\mathbf{n}\times\nabla_\Gamma\left[k-\eta Z_0\left(1+\frac{\Delta_\Gamma}{k_\varepsilon^2}\right)^{1/2}_{p,\theta}\right]^{-1}\left(1+\frac{\Delta_\Gamma}{k_\varepsilon^2}\right)^{1/2}_{p,\theta}\Pi_{\mathrm{loop}}\cdot,
\end{aligned} \tag{2.42a}$$

$$\mathbf{Y}_M=-\mathbf{n}\times\mathrm{Id}-\eta Z_0\mathbf{Y}_J, \tag{2.42b}$$

where $(1+\Delta_\Gamma/k_\varepsilon^2)^{1/2}_{p,\theta}$ is given with the help of (2.39).

In the section entitled "Finite Element Approximation", we will see how to numerically compute this operator.

Remark 2.2. In the paper [30], we have proved, in the context of the smooth surfaces, that the chosen regularized operator leads to a well posed problem (2.20) which is in fact a compact perturbation of the identity.

3 Two classical formulations for the Leontovitch condition

In this section, we briefly present two classical integral equations used to solve this kind of problem and which will allow us to evaluate the performances of the previous GCSIE.

3.1 EFIE like formulation-formulation with two unknowns [21]

This first formulation is constructed from the trace formulae (2.14)

$$\begin{cases} iZ_0\mathrm{T}\mathbf{J}(x)+\mathrm{K}\mathbf{M}(x)-\dfrac{1}{2}\mathbf{n}\times\mathbf{M}(x)=0, \\ \mathrm{K}\mathbf{J}(x)-iZ_0^{-1}\mathrm{T}\mathbf{M}(x)-\dfrac{1}{2}\mathbf{n}\times\mathbf{J}(x)=0. \end{cases} \tag{3.1}$$

Next, we introduce, in this equation, the impedance condition in the terms $\mathbf{n}\times\mathbf{M}/2$ and $\mathbf{n}\times\mathbf{J}/2$:

$$\begin{cases} iZ_0\mathrm{T}\mathbf{J}(x)+\mathrm{K}\mathbf{M}(x)-\dfrac{1}{2}\eta(x)Z_0\mathbf{J}(x)=\dfrac{1}{2}\mathbf{g}(x), \\ \mathrm{K}\mathbf{J}(x)-iZ_0^{-1}\mathrm{T}\mathbf{M}(x)+\dfrac{1}{2\eta(x)Z_0}\mathbf{M}(x)=-\dfrac{1}{2\eta(x)Z_0}\mathbf{n}\times\mathbf{g}(x). \end{cases} \tag{3.2}$$

Reciprocally, let the currents $\mathbf{J}$ and $\mathbf{M}$ solve the system (3.2). The electromagnetic field $(\mathbf{E},\mathbf{H})$ is defined by

$$\begin{cases} \mathbf{E}(x)=iZ_0\tilde{\mathrm{T}}\mathbf{J}(x)+\tilde{\mathrm{K}}\mathbf{M}(x), & x\in\Omega^+, \\ \mathbf{H}(x)=-\tilde{\mathrm{K}}\mathbf{J}(x)+iZ_0^{-1}\tilde{\mathrm{T}}\mathbf{M}(x), & x\in\Omega^+, \end{cases} \tag{3.3}$$

verifies Eqs. (2.1), (2.2) and (2.3).

Finally by the change of unknown, $\mathbf{M}/iZ_0$ becomes $\mathbf{M}$ in order to homogenize the equations, one obtains:

$$\begin{cases} \mathrm{K}\mathbf{M}+\mathrm{T}\mathbf{J}+\dfrac{i}{2}\eta\mathbf{J}=\dfrac{1}{2iZ_0}\mathbf{g}, \\ \mathrm{T}\mathbf{M}+\mathrm{K}\mathbf{J}+\dfrac{i}{2\eta}\mathbf{M}=-\dfrac{1}{2\eta Z_0}\mathbf{n}\times\mathbf{g}. \end{cases} \tag{3.4}$$

Now, (3.4) can be equivalently written under the following weak formulation: find $(\mathbf{M},\mathbf{J})\in X\times X$ ($X:=\mathbf{H}_\times^{-1/2}(\mathrm{div}_\Gamma,\Gamma)\cap\mathbf{L}_T^2(\Gamma)$) such that

$$a((\mathbf{M},\mathbf{J});(\mathbf{M}',\mathbf{J}'))=l(\mathbf{M}',\mathbf{J}'),\quad\forall(\mathbf{M}',\mathbf{J}')\in X\times X, \tag{3.5}$$

where

$$\begin{aligned} a((\mathbf{M},\mathbf{J});(\mathbf{M}',\mathbf{J}'))=&B\left(\begin{bmatrix}\mathbf{n}\times K & \mathbf{n}\times T\\ \mathbf{n}\times T & \mathbf{n}\times K\end{bmatrix}\begin{bmatrix}\mathbf{M}\\ \mathbf{J}\end{bmatrix};\begin{bmatrix}\mathbf{M}'\\ \mathbf{J}'\end{bmatrix}\right)\\ &+\frac{i}{2}\int_\Gamma\left\{\eta\mathbf{J}\cdot\mathbf{J}'+\eta^{-1}\mathbf{M}\cdot\mathbf{M}'\right\}d\Gamma, \end{aligned} \tag{3.6}$$

where the bilinear form B is defined by

$$B\left(\begin{bmatrix}\mathbf{M}\\ \mathbf{J}\end{bmatrix};\begin{bmatrix}\mathbf{M}'\\ \mathbf{J}'\end{bmatrix}\right)=-b(\mathbf{M},\mathbf{J}')+b(\mathbf{M}',\mathbf{J}) \tag{3.7}$$

with b as the extension of the bilinear form $(\mu,\nu)\in\mathbf{L}_T^2(\Gamma)\times\mathbf{L}_T^2(\Gamma)\mapsto\int_\Gamma\mu\cdot(\nu\times\mathbf{n})d\Gamma$ to the space $\mathbf{H}_\times^{-1/2}(\mathrm{div}_\Gamma,\Gamma)$ [8] (with respect to b, $\mathbf{H}_\times^{-1/2}(\mathrm{div}_\Gamma,\Gamma)$ becomes its own dual) and

$$l((\mathbf{J}',\mathbf{M}'))=\frac{1}{2}\int_\Gamma\left(\frac{\mathbf{g}}{iZ_0}\cdot\mathbf{J}'-\mathbf{n}\times\mathbf{g}\cdot\mathbf{M}'\right)d\Gamma.$$

The advantages of this formulation are:

- We can prove that the weak formulation is well-posed for any frequency. This result can be in the thesis of V. Lange [21] in the context of smooth surfaces and we can extend it for the Lipschitz polyhedron by using the inf-sup condition for the first term of the bilinear form a derived in [8].
- We can consider a conformal finite element approximation of (3.5) by considering the classical lowest-order Raviart-Thomas discrete space X_h, i.e., find $(\mathbf{M}_h,\mathbf{J}_h)\in X_h\times X_h$ such that

$$a((\mathbf{M}_h,\mathbf{J}_h);(\mathbf{M}_h',\mathbf{J}_h'))=l(\mathbf{M}_h',\mathbf{J}_h'),\quad\forall(\mathbf{M}_h',\mathbf{J}_h')\in X_h\times X_h. \tag{3.8}$$

  In particular, we can prove that the convergence of the method is quasi-optimal [8].

Remark 3.1. These advantages make this method an efficient tool to obtain an accurate solution. We use it to compute a reference solution.

The main drawbacks are:

- The two currents are used as unknowns, while an explicit relationship between them exists. So upon discretization, the size of the linear system is twice as large as in the perfect conductor case.
- The linear system is inverted by means of an iterative solver coupled with the multilevel fast multipole method noted in what follows by MFMM. The CPU time to obtain the solution is then of order $n_{iter}N\log N$ where n_{iter} is the iteration number and N is the unknown number. It is possible to perform the matrix-vector multiplication using the MFMM algorithm only two times by changing the definition of unknowns, and the numerical integration formulae. Nevertheless, the iteration number n_{iter} may be very large. Moreover, on the perfectly metallic part of the surface Γ, this formulation degenerates into a well-known equation: the Electric Field Integral Equation. It is for the reason that in following we note this formulation as the EFIE-like formulation.

3.2 CFIE-like formulation with one unknown

To overcome the main drawbacks of the EFIE-like equation that gives rise to ill-conditioned systems upon discretization, we have recently proposed a new integral method by using a Combined field Integral Equation (CFIE) approach [14]. The construction of the CFIE in the context of an impedance condition is not straightforward. Indeed, by eliminating the magnetic current $\mathbf{M}$ from the impedance condition, the interior trace formulae lead to the classical EFIE and MFIE:

$$-\mathbf{n}\times((\mathbf{E}^{\text{inc}})_{|\Gamma}\times\mathbf{n})=-\frac{1}{2}\eta Z_0\mathbf{J}-\mathrm{K}\eta Z_0\mathbf{n}\times\mathbf{J}+iZ_0\mathrm{T}\mathbf{J}, \tag{3.9a}$$

$$-\mathbf{n}\times(\mathbf{H}^{\text{inc}})_{|\Gamma}=\frac{1}{2}\mathbf{J}+\mathbf{n}\times\mathrm{K}\mathbf{J}+\mathrm{T}\eta\mathbf{n}\times\mathbf{J}. \tag{3.9b}$$

Now, assume that the impedance operator is constant. So the natural functional space to construct the weak formulation is $Z=\mathbf{H}_{\times}^{-1/2}(\mathrm{div}_{\Gamma},\Gamma)\cap\mathbf{H}_{\times}^{-1/2}(\mathrm{curl}_{\Gamma},\Gamma)$. The difficulty appears when we want to approximate the problem by a finite element method. For that we have to choose a finite dimensional space Z_h for which the weak formulation is well defined. The natural choice is to consider a conformal approximation i.e., $Z_h\subset Z$. Unfortunately, this implies that the elements of Z_h are tangential vector fields of Γ with both the flux and tangential continuity through the edges of the mesh. To our knowledge, the kind of boundary finite element space is difficult to define for a polyhedron. So, a direct elimination of the magnetic current via the impedance condition must not be used to construct an integral equation for the Leontovitch condition.

Nevertheless, it seems interesting to construct a CFIE approach for the impedance case in order to obtain good convergence behavior. As for the EFIE-like formulation, we use a simple combination of (2.14) and (2.3) to derive our Impedance Combined Field Integral Equation formulation. More precisely, we normalize (2.14a) by iZ_0 then apply a rotation of $\pi/2$ around the normal to (2.14b) and we make a linear combination of these two equations

$$\begin{aligned}&-\frac{1}{iZ_0}(\mathbf{n}\times(\mathbf{E}^{\text{inc}})_{|\Gamma}\times\mathbf{n})(x)+\gamma(\mathbf{H}^{\text{inc}})_{|\Gamma}\times\mathbf{n})(x)\\&=\Big(T\mathbf{J}(x)+K\mathbf{M}(x)-\frac{1}{2}\mathbf{n}\times\mathbf{M}(x)\Big)+\gamma\Big(\mathbf{n}\times K\mathbf{J}(x)+\mathbf{n}\times T\mathbf{M}(x)+\frac{1}{2}\mathbf{J}(x)\Big).\end{aligned} \tag{3.10}$$

The impedance condition should be added: $0=i\eta\mathbf{J}+\mathbf{n}\times\mathbf{M}$.

If we note $A_{cfie}^{\xi}=T+\xi\mathbf{n}\times K+\xi/2$ the classical integral operator for the CFIE in the metallic case, Eq. (3.10) can be written in form:

$$\begin{cases}-\dfrac{\mathbf{E}_t^{\text{inc}}}{iZ_0}+\beta\mathbf{n}\times\mathbf{H}_t^{\text{inc}}=A_{cfie}^{\beta}\mathbf{J}+\beta\mathbf{n}\times A_{cfie}^{\frac{-1}{\beta}}\mathbf{M},\\ 0=i\eta\mathbf{J}+\mathbf{n}\times\mathbf{M}.\end{cases} \tag{3.11}$$

This form is particularly interesting from the numerical point of view. Note that after discretization, it is easy to compute a matrix-vector product $A_{cfie}^{\beta}\mathbf{J}$ and $A_{cfie}^{-\beta^{-1}}\mathbf{M}$, using two times, the FMM algorithm applied to the "classical" CFIE equation.

The main difficulty of the integral formulation is knowing how to eliminate the magnetic current and more generally how to treat the rotation operator $\mathbf{n}\times\cdot$? We have proposed in [14] to keep the magnetic current as an intermediate variable and not to directly evaluate the term $\mathbf{n}\times CFIE(\mathbf{M})$. The system could be rewritten for instance in the form:

$$\begin{cases} -\dfrac{\mathbf{E}_t^{\text{inc}}}{iZ_0}+\beta\mathbf{n}\times\mathbf{H}_t^{\text{inc}}=\Big(T+\beta\mathbf{n}\times K+\dfrac{\beta}{2}\Big)\mathbf{J}+\beta\mathbf{n}\times\mathcal{V}, & \text{(a1)} \\ \mathcal{V}=\Big(T-\dfrac{1}{\beta}\mathbf{n}\times K-\dfrac{1}{2\beta}\Big)\mathbf{M}, & \text{(b1)} \\ \mathbf{n}\times\mathbf{M}=-i\eta\mathbf{J}. & \text{(c1)} \end{cases} \tag{3.12}$$

The term $(T-\beta^{-1}\mathbf{n}\times K-(2\beta)^{-1})\mathbf{M}$ is easy to discretize because it corresponds to a classical CFIE term. We have determined an approximate of its composition with $\mathbf{n}\times\cdot$ by using a discrete Helmholtz decomposition (see [14] for more details). An other solution is possible; we can use the barycentric finite element space proposed by S. Christiansen and A. Buffa [9] which allows an uniform inf-sup stable discretization of (3.12)-(c1). This solution has been investigated in [29].

To sum up, we have in the previous sections, briefly outlined the construction of three kinds of Integral equation formulations: the EFIE-like equation (see Section (3.1)), the CFIE-like equation (see Section (3.2)) and the GCSIE equation (see Section (2.2)). The next section describes quickly the discretization of these integral equations but also all useful numerical tools.

4 Finite element approximations

In this section, we explain how to approximate the integral equations by using a finite element approach. Our goal is to solve iteratively the linear system by using a GMRES (Generalized Minimal Residual Method) solver. In this case, we have to be able to compute the matrix-vector product at each iteration.

4.1 Finite element spaces

One considers a conformal triangulation $\mathscr{T}_h$ composed of triangles of the surface Γ [12]. The approximations $\mathbf{u}_h$, $\mathbf{J}_h$ and $\mathbf{M}_h$ of the density $\tilde{g}$ and the currents $\mathbf{J}$ and $\mathbf{M}$ are searched in the lowest order Raviart-Thomas finite element space RT_0 defined by:

$$\text{RT}_0=\left\{\mathbf{v}_h\in\text{H}^0(\text{div}_\Gamma,\Gamma):\forall T\in\mathscr{T}_h,\mathbf{v}_{h|T}\circ F_T=\begin{pmatrix} a \\ b \end{pmatrix}+d\begin{pmatrix} \hat{x} \\ \hat{y} \end{pmatrix},\ \text{for}\ \ a,b,c\in\text{IR}\right\}, \tag{4.1}$$

where $\mathrm{H}^0(\mathrm{div}_\Gamma,\Gamma)=\{\mathbf{v}_h\in \mathrm{L}^2_T(\Gamma):\mathrm{div}_\Gamma \mathbf{v}_h\in \mathrm{L}^2(\Gamma)\}$ with $\mathrm{L}^2_T(\Gamma)$ be the set of tangential vector fields to Γ which are square integrable and F_T is the mapping defined by:

$$F_T:\hat{T}=\{(\hat{x},\hat{y}):0\leq\hat{x},\hat{y}\leq 1 \text{ and } \hat{y}\leq 1-\hat{x}\}\to T, \tag{4.2a}$$

$$(\hat{x},\hat{y})\to S_1^T(1-\hat{x}-\hat{y})+S_2^T\hat{x}+S_3^T\hat{y} \text{ with } S_1^T,S_2^T,S_3^T \text{ the vertices of } T. \tag{4.2b}$$

This space are described by the following basis functions: let A be an edge of the mesh $\mathscr{T}_h$ such that $A=T\cap T'$ for $T,T'\in\mathscr{T}_h$ and we denote by S and S' the vertices of T and T' respectively which don't belong to A. One associates to each edge A the basis function $\varphi_A\in \mathrm{RT}_0$ defined by

$$\varphi_A(M)=\begin{cases}\dfrac{S\vec{M}}{2|T|} \text{ for } M\in T,\\ -\dfrac{S'\vec{M}}{2|T'|} \text{ for } M\in T',\end{cases} \tag{4.3}$$

where $|T|$ is the area of the triangle $T\in\mathscr{T}_h$.

So, the dimension of RT_0 is equal to the number of edges in the mesh. For the approximation of $\mathbf{Y}_J$, we will need the following spaces:

$$\mathscr{P}^{1,c}(\mathscr{T}_h)=\{v_h\in \mathrm{C}^0(\Gamma):\forall T\in\mathscr{T}_h,\ v_{h|T}\circ F_T=a+b\hat{x}+c\hat{y} \text{ for } a,b,c\in\mathbb{R}\}, \tag{4.4a}$$

$$\overset{\circ}{\mathscr{P}}{}^{1,c}(\mathscr{T}_h)=\left\{v_h\in\mathscr{P}^{1,c}(\mathscr{T}_h):\int_\Gamma v_h d\Gamma=0\right\}. \tag{4.4b}$$

The first space is the classical space of continuous and piecewise linear functions associated to the nodes of the mesh and the second one is the subspace of $\mathscr{P}^{1,c}(\mathscr{T}_h)$ which contains the functions whose mean value on Γ is zero. This last space is used to compute the potentials associated to the Helmholtz decomposition which are defined up to a constant.

4.2 Approximation of the operators T and K

The discretization of the integral operators T and K is well-known and is based on variational formulations. The bilinear forms associated to the operators T and K are respectively: $\forall J^t(x)\in\mathbf{H}_\times^{-1/2}(\mathrm{div}_\Gamma,\Gamma)$

$$\langle TJ,J^t\rangle\int_\Gamma\int_\Gamma kG(x,y)(J(y)\cdot\overline{J^t}(x)-\frac{1}{k^2}\mathrm{div}_\Gamma J(y)\overline{\mathrm{div}_\Gamma J^t}(x))d\Gamma(y)d\Gamma(x), \tag{4.5a}$$

$$\langle KJ,J^t\rangle=\int_\Gamma\int_\Gamma(\nabla_y G(x,y)\times J(y))\cdot\overline{J^t(x)\times\mathbf{n}(x)}d\Gamma(x). \tag{4.5b}$$

Next, one uses conformal finite element approximation of the $\mathbf{H}_\times^{-1/2}(\mathrm{div}_\Gamma,\Gamma)$ by using the Raviart-Thomas space and one constructs the matrices associated to the previous bilinear forms by using the basis functions (4.3). The size of each system is equal to $3/2$ times the numbers of triangles in the mesh.

4.3 Discretization of $\mathbf{Y}_J$

In this section, we describe an approximation of the action of the operator $\mathbf{Y}_J$. In other worlds, we want to compute an approximation $\mathbf{Y}_J^h\mathbf{u}_h$ of $\mathbf{Y}_J\mathbf{u}_h$ for $\mathbf{u}_h \in \mathrm{RT}_0$. This approximation must be sought in RT_0 because we want to apply it the operator T (see (2.20)). Let $\mathbf{u}^h$ be an element of RT_0. The action of $\mathbf{Y}_J$ on $\mathbf{u}^h$ needs four steps. The following diagram formally describes these four steps which are detailed just after.

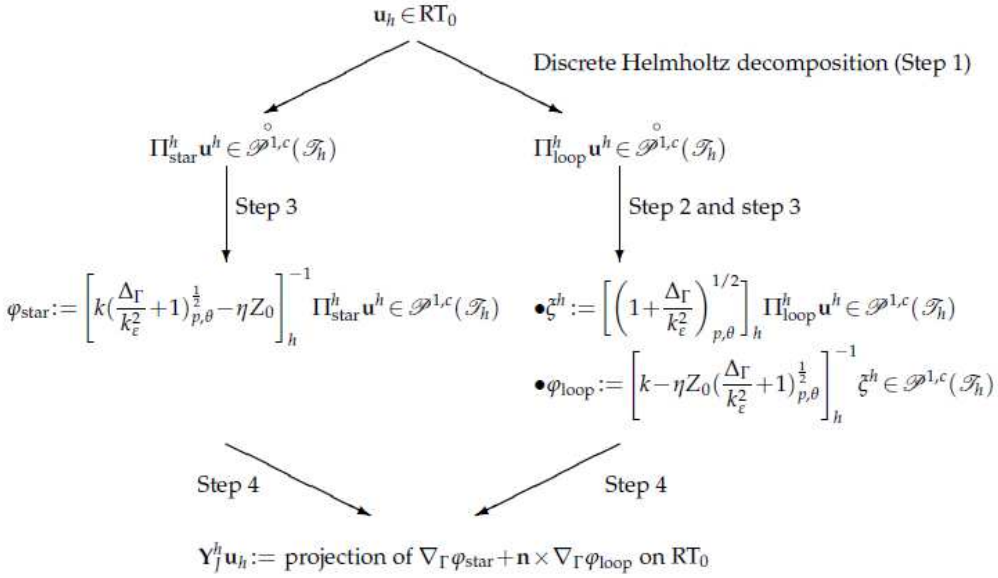

- First step: **Calculation of $\Pi^h_{\mathbf{star}}\mathbf{u}^h$ and $\Pi^h_{\mathbf{loop}}\mathbf{u}^h$.**

  For that, we note that Π_{star} and Π_{loop} can be characterized by: let $\mathbf{u} = (\mathbf{n}\times\nabla\Pi_{\mathrm{loop}} + \nabla\Pi_{\mathrm{star}})\mathbf{u}$ be the Helmholtz decomposition of $\mathbf{u}$. So, we immediately have:

  $$\mathrm{curl}_\Gamma\mathbf{u} = \mathrm{curl}_\Gamma\mathbf{n}\times\nabla\Pi_{\mathrm{loop}}\mathbf{u} = -\Delta_\Gamma\Pi_{\mathrm{loop}}\mathbf{u}, \tag{4.6a}$$

  $$\mathrm{div}_\Gamma\mathbf{u} = \mathrm{div}_\Gamma\nabla\Pi_{\mathrm{star}}\mathbf{u} = \Delta_\Gamma\Pi_{\mathrm{star}}\mathbf{u}, \tag{4.6b}$$

  where curl_Γ is the adjoint operator of $\mathbf{n}\times\nabla_\Gamma$, which is defined by $\int_\Gamma \mathrm{curl}_\Gamma\mathbf{u}v d\Gamma = \int_\Gamma \mathbf{u}\cdot\mathbf{n}\times\nabla_\Gamma v d\Gamma$ with $\mathbf{u}$ be a tangential vector field to Γ and v be a scalar function defined on Γ.

  Since the potentials $\Pi_{\mathrm{loop}}\mathbf{u}$ and $\Pi_{\mathrm{star}}\mathbf{u}$ are defined modulo a constant, we choose to approximate them by a finite element method by considering the following discrete weak formulations:

  – find $\Pi^h_{\mathrm{star}}\mathbf{u}^h \in \mathring{\mathscr{P}}^{1,c}(\mathscr{T}_h)$ the solution of: $\forall\varphi_h \in \mathring{\mathscr{P}}^{1,c}(\mathscr{T}_h)$

  $$\int_\Gamma \nabla_\Gamma\Pi^h_{\mathrm{star}}\mathbf{u}^h\cdot\nabla_\Gamma\varphi_h d\Gamma = \int_\Gamma \mathbf{u}_h\cdot\mathbf{n}\times\nabla_\Gamma\varphi_h d\Gamma, \tag{4.7}$$

– and find $\Pi^h_{\text{loop}}\mathbf{u}^h \in \overset{\circ}{\mathscr{P}}{}^{1,c}(\mathscr{T}_h)$ the solution of: $\forall \varphi_h \in \overset{\circ}{\mathscr{P}}{}^{1,c}(\mathscr{T}_h)$

$$\int_\Gamma \nabla_\Gamma \Pi^h_{\text{loop}}\mathbf{u}^h \cdot \nabla_\Gamma \varphi_h d\Gamma = -\int_\Gamma \text{div}_\Gamma \mathbf{u}_h \varphi_h d\Gamma. \tag{4.8}$$

Eqs. (4.7) and (4.8) induce two sparse linear systems:

$$\text{RU}_{\text{star}} = \text{L}^{\mathbf{u}_h}_{\text{star}} \quad \text{and} \quad \text{RU}_{\text{loop}} = \text{L}^{\mathbf{u}_h}_{\text{loop}}, \tag{4.9}$$

where R is the stiffness matrix associated to the basis functions of the space $\overset{\circ}{\mathscr{P}}{}^{1,c}(\mathscr{T}_h)$, U_{star} and U_{loop} are the associated degrees of freedom and $\text{L}^{\mathbf{u}_h}_{\text{star}}$ and $\text{L}^{\mathbf{u}_h}_{\text{loop}}$ are the right hand sides corresponding to the vectors $(\int_\Gamma \mathbf{u}_h \cdot \mathbf{n} \times \nabla_\Gamma \psi_i d\Gamma)^T_i$ and $(-\int_\Gamma \text{div}_\Gamma \mathbf{u}_h \psi_i d\Gamma)^T_i$ respectively with ψ_i being the basis functions of the finite element space $\overset{\circ}{\mathscr{P}}{}^{1,c}(\mathscr{T}_h)$.

- Second step: **Calculation of the action of** $(\Delta_\Gamma/k_\varepsilon^2+1)^{1/2}_{p,\theta}$**.**

Let ξ be a scalar function defined on Γ. The action of the operator $(\Delta_\Gamma+k^2)^{1/2}_{p,\theta}$ on ξ can be decomposed in the following way:

– Calculation of $\xi_j=(1+B^p_j(\theta)\Delta_\Gamma/k_\varepsilon^2)^{-1}\xi$ for $j=1,\cdots,p$, which can be also written in the form: find ξ_i be the solution of

$$\left(1+B^p_j(\theta)\frac{\Delta_\Gamma}{k_\varepsilon^2}\right)\xi_j = \xi. \tag{4.10}$$

As previously, this problem can be solved by a finite element method. In particular, we have used the discrete problem: find $\xi^h_j \in \mathscr{P}^{1,c}(\mathscr{T}_h)$ such that $\forall \xi' \in \mathscr{P}^{1,c}(\mathscr{T}_h)$

$$\int_\Gamma \xi^h_j \xi' d\Gamma - \frac{B^p_j(\theta)}{k_\varepsilon^2}\int_\Gamma \nabla\xi^h_j \cdot \nabla\xi' d\Gamma = \int_\Gamma \xi\xi' d\Gamma. \tag{4.11}$$

Eq. (4.11) may be written as a linear system:

$$\text{A}^j_{p,\theta}\Xi_j = \text{L}^\xi, \quad \text{for } j=1,\cdots,p. \tag{4.12}$$

– Approximation of $A^p_0(\theta)\xi+\sum_{j=1}^p A^p_j(\theta)(\Delta_\Gamma/k_\varepsilon^2)\xi_j$ can also be achieved by using a finite element method: find $[(1+\Delta_\Gamma/k_\varepsilon^2)^{1/2}_{p,\theta}]_h\xi \in \mathscr{P}^{1,c}(\mathscr{T}_h)$ such that $\forall \xi' \in \mathscr{P}^{1,c}(\mathscr{T}_h)$:

$$\int_\Gamma \left[\left(1+\frac{\Delta_\Gamma}{k_\varepsilon^2}\right)^{1/2}_{p,\theta}\right]_h \xi\xi' d\Gamma = A^p_0(\theta)\int_\Gamma \xi\xi' d\Gamma - \sum_{j=1}^p \frac{A^p_j(\theta)}{k_\varepsilon^2}\int_\gamma \nabla\xi^h_j \cdot \nabla\xi' d\Gamma. \tag{4.13}$$

If we note $S^{\xi}_{p,\theta}$ the degrees of freedom associated to $[(1+\Delta_\Gamma/k_\varepsilon^2)^{1/2}_{p,\theta}]_h\xi$, (4.13) corresponds to the solution of the sparse linear system:

$$MS^{\xi}_{p,\theta} = A_0^p(\theta)L^{\xi} - \sum_{j=1}^{p} \frac{A_j^p(\theta)}{k_\varepsilon^2} R\Xi_j, \tag{4.14}$$

where M is the mass matrix of the space $\mathscr{P}^{1,c}(\mathscr{T}_h)$.

In conclusion, the approximation of the action of $(\Delta_\Gamma+k^2)^{1/2}_{p,\theta}$ on $\Pi^h_{\text{star}}\mathbf{u}$ corresponds to:

$$S^{\xi}_{p,\theta} = A_0^p L^{\xi} + M^{-1}\left(\sum_{j=1}^{p} \frac{A_j^p(\theta)}{k_\varepsilon^2} R\left(A^j_{p,\theta}\right)^{-1} L^{\xi}\right). \tag{4.15}$$

- Third step: **Calculation of the action** $[k(\Delta_\Gamma/k_\varepsilon^2+1)^{1/2}_{p,\theta}-\eta Z_0]^{-1}$ **and** $[k-\eta Z_0(\Delta_\Gamma/k_\varepsilon^2+1)^{1/2}_{p,\theta}]^{-1}$.
  Let ξ be a scalar function defined on Γ. The action of the operator $[k(\Delta_\Gamma/k_\varepsilon^2+1)^{1/2}_{p,\theta}-\eta Z_0]^{-1}$ on ξ can be decomposed in the following augmented system: find ϕ such that

$$\begin{cases} (kA_0^p-\eta Z_0)\phi + k\displaystyle\sum_{j=1}^{p} A_j^p(\theta)\frac{\Delta_\Gamma}{k_\varepsilon^2}\xi_j = \xi, \\ \left(1+B_j^p(\theta)\dfrac{\Delta_\Gamma}{k_\varepsilon^2}\right)\xi_j - \phi = 0, \quad \forall p=1,\cdots,p. \end{cases} \tag{4.16}$$

  As previously, we can write this system under a weak formulation and discretize it by using a finite element method in $\mathscr{P}^{1,c}(\mathscr{T}_h)$. We obtain an approximation of the action of $[k-\eta Z_0(\Delta_\Gamma/k_\varepsilon^2+1)^{1/2}_{p,\theta}]^{-1}$ with the same approach. In what follows, we note $[k(\Delta_\Gamma/k_\varepsilon^2+1)^{1/2}_{p,\theta}-\eta Z_0]^{-1}_h\xi \in \mathscr{P}^{1,c}(\mathscr{T}_h)$ and $[k-\eta Z_0(\Delta_\Gamma/k_\varepsilon^2+1)^{1/2}_{p,\theta}]^{-1}_h\xi \in \mathscr{P}^{1,c}(\mathscr{T}_h)$ the results of these approximations.

- Fourth step: **Calculation of L^2 projection**.
  Finally, in order to use the classical approximations of integral operators, the action $\mathbf{Y}_J$ must be in RT_0. For that, we simply make the L^2 projection of the decomposition $\mathbf{n}\times\nabla\xi_1^h+\nabla\xi_2^h$ where ξ_1^h, $\xi_2^h \in \mathscr{P}^{1,c}(\mathscr{T}_h)$ on RT_0. This induces the two problems: let $\xi^h \in \mathscr{P}^{1,c}(\mathscr{T}_h)$, find $\mathbf{v}^h_{\text{loop}} \in RT_0$ such that

$$\int_\Gamma \mathbf{v}^h_{\text{loop}}\cdot\mathbf{w}^h d\Gamma = \int_\Gamma \mathbf{n}\times\nabla\xi^h\cdot\mathbf{w}^h d\Gamma, \quad \forall \mathbf{w}^h \in RT_0, \tag{4.17}$$

  and find $\mathbf{v}^h_{\text{star}} \in RT_0$ such that

$$\int_\Gamma \mathbf{v}^h_{\text{star}}\cdot\mathbf{w}^h d\Gamma = \int_\Gamma \nabla\xi^h\cdot\mathbf{w}^h d\Gamma, \quad \forall \mathbf{w}^h \in RT_0, \tag{4.18}$$

or in the matrix form

$$\mathrm{V}_{\mathrm{loop}} = M_{\mathrm{RT}}^{-1}\mathrm{P}_{\mathrm{loop}}^{\mathrm{RT}}\Xi^h \quad \text{and} \quad \mathrm{V}_{\mathrm{star}} = M_{\mathrm{RT}}^{-1}\mathrm{P}_{\mathrm{star}}^{\mathrm{RT}}\Xi^h, \tag{4.19}$$

where $\mathrm{V}_{\mathrm{loop}}$ and $\mathrm{V}_{\mathrm{star}}$ are respectively the degrees of freedom associated to $\mathbf{v}_{\mathrm{loop}}^h$ and $\mathbf{v}_{\mathrm{star}}^h$, M_{RT} is the mass matrix of RT_0, $\mathrm{P}_{\mathrm{loop}}^{\mathrm{RT}}$ is the matrix corresponding to the integrals $\int_\Gamma \mathbf{n}\times\nabla\xi^h\cdot\mathbf{w}^h d\Gamma$ and $\mathrm{P}_{\mathrm{star}}^{\mathrm{RT}}$ the one corresponding to $\int_\Gamma \nabla\xi^h\cdot\mathbf{w}^h d\Gamma$.

Finally, we define the approximation $\mathbf{Y}_J^h$ of the operator $\mathbf{Y}_J$ as:

$$\begin{aligned}
&\mathbf{Y}_J^h : \mathrm{RT}_0 \to \mathrm{RT}_0\\
&\mathbf{u}^h \mapsto \mathcal{P}^{\mathrm{RT}}\nabla_\Gamma\left[k\Big(\frac{\Delta_\Gamma}{k_\varepsilon^2}+1\Big)_{p,\theta}^{\frac{1}{2}} - \eta Z_0\right]_h^{-1}\Pi_{\mathrm{star}}^h\mathbf{u}^h\\
&\qquad + \mathcal{P}^{\mathrm{RT}}\mathbf{n}\times\nabla_\Gamma\left[k-\eta Z_0\Big(\frac{\Delta_\Gamma}{k_\varepsilon^2}+1\Big)_{p,\theta}^{\frac{1}{2}}\right]_h^{-1}\left[\Big(1+\frac{\Delta_\Gamma}{k_\varepsilon^2}\Big)_{p,\theta}^{1/2}\right]_h\Pi_{\mathrm{loop}}^h\mathbf{u}^h,
\end{aligned} \tag{4.20}$$

where $\mathcal{P}^{\mathrm{RT}}$ denotes the L^2 projection on the RT_0 finite element space.

5 Numerical results

To sum up, we have in the previous sections, briefly outlined the construction of three kinds of integral formulations:

- **The EFIE-like equation:** The main advantage of this formulation is the accuracy of the solution. On the contrary, the drawback is that the convergence rate is very slow and sometimes the solution can not be obtained.
- **The CFIE-like equation:** This formulation is conversely opposite to the previous one. Because, its convergence rate is normally very good but solutions are sometimes inaccurate. This CFIE-like formulation is not applicable to open surfaces.
- **The GCSIE equation:** This formulation is intrinsically well-conditioned and no preconditioner is needed.

In this section, we give some numerical experiments to compare the three approaches and to deduce the advantages from each compared to the others. We focus also on the ability of the new integral equation (see Section 2.2) to effectively solve scattering problem specially when an impedance condition is imposed. To begin with, we will define the accuracy of the three methods by comparing solutions with analytical results. Next, the convergence rate is analyzed, specially the influence of the discretization on the number of iterations is studied. At the end, we look at non academic cases.

All objects are located in free space. Let us recall that for all types of integral equations, the matrix-vector multiplication is performed by using only twice times the MFMM

algorithm. For all numerical cases, the linear system is solved by using an GMRES solver (see [20]). In the case of the EFIE/CFIE-like formulation, to speed up the convergence of the iterative solver, we construct a right SParse Approximate Inverse preconditioner (see for example [10, 11]). Let us make some remarks. The CPU time needed to obtain the solution noted t_{cpu} is the sum of two terms: one linked to the time needed to reach the solution t_{iter} which is of order $t_{iter} = n_{iter} 2N \log N$ plus eventually the time due to the construction of the preconditioner t_{pre}.

All geometries are triangulated with a mesh size of about $\lambda/10$ except when it is indicated. The number of level FMM level Lv is fixed as the size of the small box is equal to $1.5/k$. We suppose that convergence is reached when the residue is equal to 10^{-4}. When it is not possible to obtain such a residue, convergence is stopped after 300 iterations and we indicate the obtained residue in parenthesis.

5.1 Memory storage

For simplicity, we analyze the memory storage in the case when a impedance condition is imposed such that η is a non zero constant. Let us analyze the memory storage due to the close interactions. We note by α the memory storage required when the EFIE formulation is used for the perfectly conducting case.

- In the impedance case, the number of unknowns has doubled. So the memory requirement for EFIE-like formulation is 2α.
- For the CFIE-like formulation, we apply twice times the FMM algorithm applied to the "classical" CFIE equation. Hence, the memory requirement is about 4α.
- The GCSIE formulation uses exactly the same MFMM algorithm as this used by EFIE-like formulation. So the memory is about 2α.

In conclusion, the close interactions require less memory when the EFIE/GCSIE formulation is used.

The other main part of the memory storage is the storage of the preconditioner when the latter is needed. The storage requirement is the same for the CFIE-like as in the perfectly conducting case. But for the EFIE-like formulation, this requirement is doubled because the number of unknowns is doubled. Recall that for the GCSIE, no preconditioner is needed. Table 1 gives an example of the memory storage in the case of the sphere. The first line of the Table 1 indicates the memory requirement in the case of perfectly conducting case. Due to the fact that the number of unknowns has doubled, the memory required for the close matrix is increased by a factor close to 2 in the case of the EFIE-like /GCSIE integral formulation. In these two cases, only the real part of the close matrix is needed to be stored. But for the CFIE-like formulation, the complex values of the close matrix are stored. So we observe that the memory requirement is increased by a factor 4. We note the same increase by a factor 4 for the storage of the preconditioner due to the same reasons. A out-of-core version has been implemented in order to reduce the memory.

Table 1: Memory storage used for a perfectly conducting sphere and for a impedance sphere.

formulation	close matrix	preconditioner
EFIE	752*Mbytes*	641*Mbytes*
EFIE-like	1.7Gbytes	2.56Gbytes
CFIE-like	5.95Gbytes	723Mbytes
GCSIE	1.7Gbytes	0

5.2 Analytical case: sphere case

In this subsection, we will analyze the efficiency of the iterative solver. The effect of the frequency and of the mesh size will be studied. To start with a comparison, we calculate the electromagnetic scattering from a sphere with radius $a=1m$. This sphere is illuminated by a plane wave given by

$$E^{inc}(x,y,z,t)=E_0e^{-i(\omega t+kz)}\hat{x}, \quad E_0=1\mathrm{Vm}^{-1}.$$

An analytical solution obtained from the Mie series may be computed.

5.2.1 Effect of the value of the frequency

Table 2 gives us the convergence rate for some values of the frequencies. We have fixed the impedance value η to be equal 1. n_{ddl} indicates the number of degrees of freedom. The number of points per wavelength is at the beginning fixed at 10. n_{iter} is the value of the number of iterations to obtain a residu fixed to 10^{-4}. If this value is not obtained after 300 iterations, the value of the residu is given. The value t_1 is the value of the CPU time

Table 2: Number of iterations for various spheres versus the frequency (the value of the impedance and the number of points per wavelength are fixed).

formulation	frequency	n_{ddl}	n_{iter}	t_1	$t_{iter}+t_{pre}$
EFIE-like	573Mhz	18000	17		$18min+12min$
CFIE-like	573Mhz	18000	10		$4min+17min$
GCSIE	573 Mhz	18000	6	$30s$	$3min$
EFIE-like	907Mhz	48000	19		$41min+33min$
CFIE-like	907Mhz	48000	11		$15min+45min$
GCSIE	907 Mhz	48000	6	$40s$	$8min$
EFIE-like	1.3Ghz	108000	22		$60min+78min$
CFIE-like	1.3Ghz	108000	12		$23min+104min$
GCSIE	1.3Ghz	108000	6	$2min$	$16min$
EFIE-like	2Ghz	216750	25		$108min+119min$
CFIE-like	2Ghz	216750	14		$56min+164min$
GCSIE	2Ghz	216750	6	$3min$	$30min$

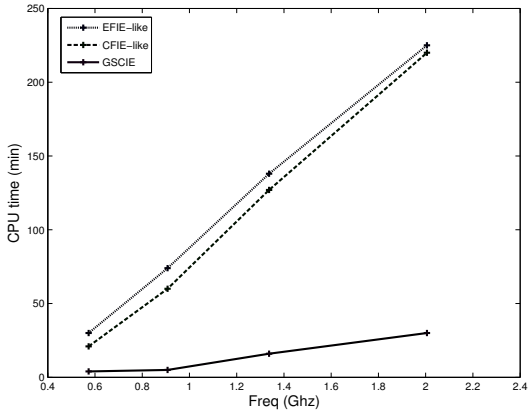

Figure 2: CPU Time versus the frequency for impedance spheres (the value of the impedance and the number of points per wavelength are fixed).

needed to extra computations to find the operators in the case of the new formulation GCSIE. The values of the CPU time is given in minutes. We remark that:

- The EFIE/CFIE solution requires more and more iterations when the frequency increases. Moreover, at high frequencies, it is difficult to reach a 10^{-4} residue for the EFIE formulation.
- The number of iterations needed when the EFIE/CFIE is greater by about a factor 2 than this needed for the GCSIE solution.
- On the contrary, the CGFIE solution is obtained after a small number of iterations. This number is practically independent of the value of the frequency.

We observe the same conclusions when the impedance value η is changed and also when it is piecewise constant.

Fig. 2 gives us the CPU time needed to obtain the solution noted t_{cpu} versus the value of the frequency. In the case of the GCSIE formulation, $t_{pre}$is equal to zero and n_{iter} seems to be very to be steady (see Table 2). We expect that t_{cpu} is close to a constant. If we look at Fig. 2, we observe a slight increase on t_{cpu}. It is due to the increase of n_{ddl} which grows up with the frequency. In the case of the EFIE/CFIE formulation, n_{iter} increases dramatically when the frequency increases. Moreover, it is the same for t_{pre}. And we observe a strong rise of t_{cpu} with the frequency (see Fig. 2 curves blue and green).

5.2.2 Accuracy

Fig. 3 shows the Radar Cross Sections obtained using the three formulations. The curves are very close to each other (see Figs. 3 and 4). An analytical reference is computed and is called the MIE solution. We evaluate the accuracy of the three methods in two ways. First, we observe the ability of the methods to compute the strong attenuation of the RCS at the zero angle. This behavior is very difficult to compute and its knowledge is

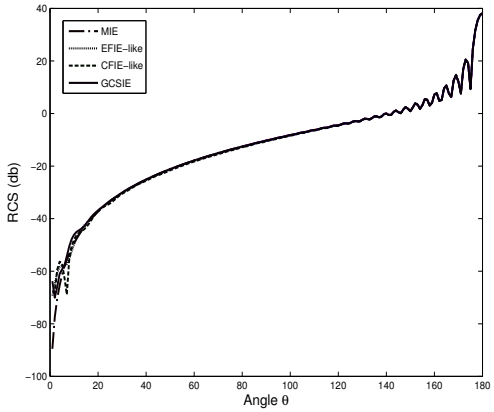

Figure 3: Radar cross section for impedance spheres when the frequency is fixed equal to 2GHz.

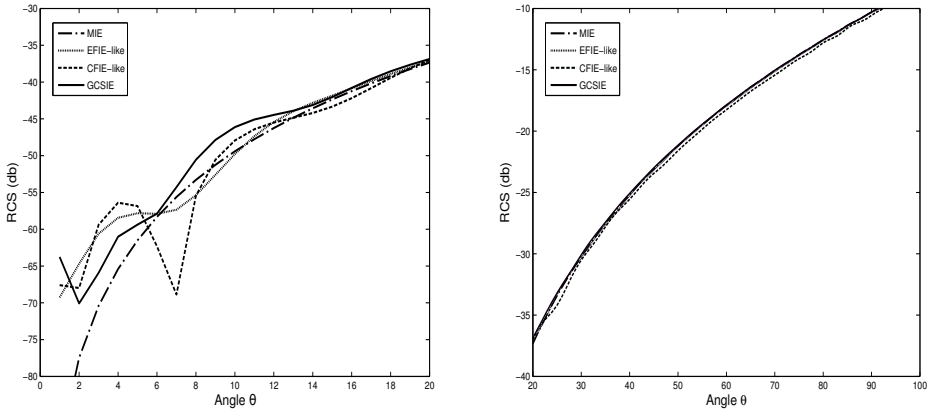

Figure 4: Zoom of the previous figure.

important in the furtivity domain for example. Fig. 4 shows some differences at the zero angle and one can see the good accuracy of the GCSIE, in particular, in comparison to the CFIE. The second way is the computation of the relative error on the RCS (without the log scale). The Table 3 shows the percentage of the relative errors on the radar cross section in the sphere case. Note that the obtained values of the relative errors are very small for all the methods. We observe that the EFIE has better accuracy whereas the GCSIE seems to be the less accurate for this kind of error measure.

Table 3: Relative errors on the radar cross section for impedance versus the value of the frequency (the value of the impedance and the number of points per wavelength are fixed).

frequency	EFIE-like	CFIE-like	GCSIE
1.3Ghz	0.03%	0.3%	1.2%
2Ghz	0.04%	0.3%	1.3%

5.2.3 Effect of the mesh size

In order to study the effect of the mesh size, we have fixed the value of the frequency to be equal to 573Mhz. and the impedance value η to be equal 1. Table 4 gives us the convergence rate for some values of the mesh size.

Table 4: Mesh refinement study for an impedance sphere versus the refinement (the value of the impedance and the frequency are fixed).

formulation	$\frac{\lambda}{h}$	n_{ddl}	n_{iter}
EFIE-like	10	18000	17
CFIE-like	10	18000	10
GCSIE	10	18000	6
EFIE-like	16	48000	17
CFIE-like	16	48000	10
GCSIE	16	48000	6
EFIE-like	25	108000	23
CFIE-like	25	108000	21
GCSIE	25	108000	7
EFIE-like	35	216750	25
CFIE-like	35	216750	23
GCSIE	35	216750	7

We remark that for the GCSIE formulation, the number of iterations is independent of the mesh size and only a small number of iterations is required to obtain the solution (of order $6-10$). For the other formulations, we observe a very small dependence on the mesh size. In fact, the number of levels in the MFMM algorithm is fixed at 5. And the number of iterations required is greater than $6-7$. The effect of the mesh size is relatively weak when the impedance is fixed to 1 (see Table 4) but it depends on the value of the impedance. For small values, we observe a increase of the rate convergence.

5.2.4 Effect of the impedance value

The case where the sphere is a sphere covered with a fine aluminum layer is considered now. The value of impedance is given by a formula of type:

$$\Re\mathfrak{e}(\eta) = \sqrt{\frac{F}{10^{-9}}} 15.610^{-3}. \tag{5.1}$$

(This formula is given to us by an industrial company). Using an model of imperfectly conducting obstacles, it is possible to deduce the value of the impedance by:

$$\eta = \sqrt{\frac{F}{10^{-9}}} 15.610^{-3}(1-\mathrm{i}).$$

Table 5: Number of iterations for various spheres versus the frequency (the value of the impedance is changed and the number of points per wavelength are fixed).

formulation	frequency	n_{ddl}	$\Re\mathfrak{e}(\eta)$	n_{iter}	t_1	$t_{iter}+t_{pre}$
EFIE-like	573Mhz	18000	0.012	17		$8min+12min$
CFIE-like	573Mhz	18000	0.012	10		$4min+17min$
GCSIE	573Mhz	18000	0.012	6	$30s$	$3min$
EFIE-like	907Mhz	48000	0.015	201		$310min+33min$
CFIE-like	907Mhz	48000	0.015	19		$28min+45min$
GCSIE	907Mhz	48000	0.015	6	$1min$	$10min$
EFIE-like	1.3Ghz	108000	0.018	$300(410^{-3})$		$600min+65min$
CFIE-like	1.3Ghz	108000	0.018	20		$40min+105min$
GCSIE	1.3Ghz	108000	0.018	6	$2min18$	$13min$
EFIE-like	2Ghz	216750	0.022	250		$941min+118min$
CFIE-like	2Ghz	216750	0.022	23		$98min+132min$
GCSIE	2Ghz	216750	0.022	6	$5min$	$30min$

Note that the value of the impedance depends now on the frequency. For each example, the number of points per wavelength is fixed to be about 10. Table 5 gives us the number of iterations for each case. We note that

- For the new formulation GCSIE:
  - The number of iterations is almost the same. It does not depend on the value of the frequency or on the value of the impedance (see Tables 5 and 2).
  - We observe the same value of the CPU time t_{iter} in Table 5 and in Table 2. This CPU time is independent of the value of the impedance. It is only linked to the CPU time needed to perform a matrix-vector product.
- For the classical formulations:
  - The number of iterations depends on the value of the frequency and also the value of the impedance.
  - The increase for the CPU time is completely linked to the increase of the number of iterations.

5.3 Industrial cases

5.3.1 Almond case: tip shaped problem

The NASA almond is a popular benchmark for codes computing the RCS. We consider the case of the NASA almond with a total length of $2.5m$ and a surface equal to $4m^2$. The incident waves illuminates the obstacle by the tip. The frequency is chosen to be fixed to 2.6Ghz. The number of triangles is 67324 and the number of nodes is 33664. The number

Table 6: Number of iterations for the impedance almond (the value of the frequency is fixed).

formulation	value of η	n_{iter}
EFIE-like	$0.025+i0.025$	139
CFIE-like	$0.025+i0.025$	18
GCSIE	$0.025+i0.025$	13

by wavelength is about 10 with an over refined mesh near the tip. Table 6 gives us the convergence rate for one value of η. We still show that the GCSIE formulation gives the solution with smaller number of iterations and requires the small amount of the CPU time to obtain the solution. Fig. 5 gives the RCS for the almond. The curves are very close to each other. We see that the GCSIE formulation allows us to obtain the accurate solution with the smallest value of the CPU time even if the obstacle has a tip.

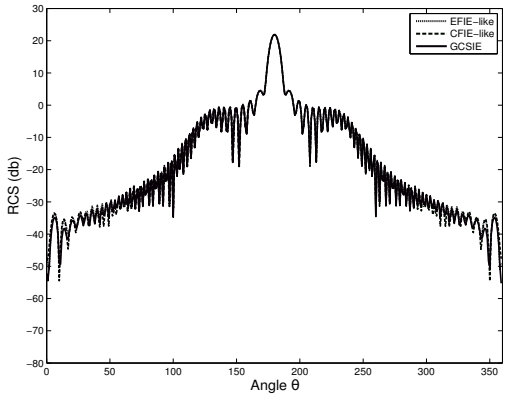

Figure 5: Radar cross section for impedance almond where the impedance is fixed to $0.025+i0.025$.

5.3.2 Channel case: cavity problem

In this section, we will investigate the scattering problem of a deep and shaped open cavity. It is well known that such a problem is often considered as a challenge in computational electromagnetics.

The frequency is fixed to be equal to 5Ghz. The exterior of the channel geometry is supposed to be metallic and in the interior, an impedance relation is imposed. The value of the impedance is fixed to $0.035+i0.035$.

Fig. 7 gives us the residue versus the number of iterations. The convergence of the solution is difficult to reach due to the cavity effect. But again, we note that the number of iterations for the GCSIE formulation is smaller than those obtained for these other integral formulations. It is of order 30 for a residue fixed to 3×10^{-3} and of order 40 for a residue fixed to 10^{-4}. For the EFIE-like formulation, as it is well known, we show a flatness effect on the convergence curve. It is mainly due to the effect of the cavity. Fig. 7 gives the RCS for the channel. The curves are very close to each other.

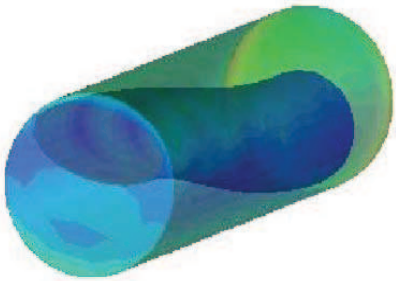

Figure 6: Geometry of the channel.

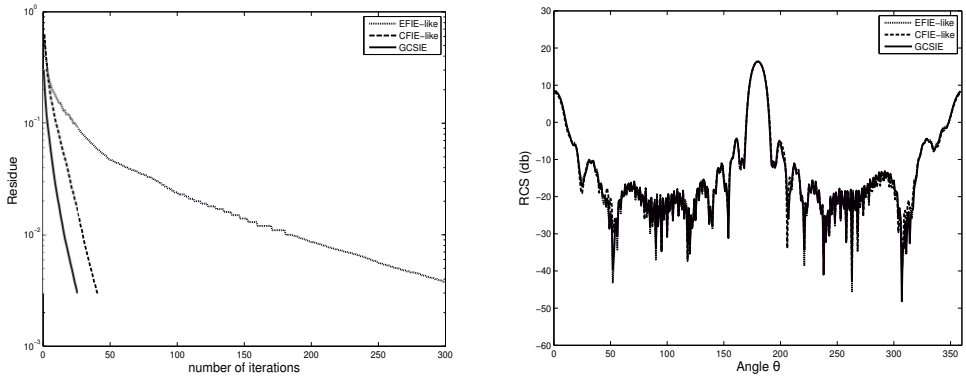

Figure 7: Residu versus the number of iterations required for the solution (left) and radar cross section (right) for impedance channel.

6 Conclusions

We have analyzed in this paper, different integral equations formulations for the scattering by 3-D arbitrary shaped objects. Besides the classical integral equations formulations (EFIE-CFIE), we have proposed to study a well-conditioned integral formulation. The foremost feature of this GCSIE is to be well-conditioned. Obtaining this integral equation and its discretization are described in detail. Numerical experiences are given. Solutions are obtained by using iterative solvers coupled with the multilevel fast multipole algorithm. We have investigated the case where a variable impedance condition is imposed at the boundary. Several numerical examples (academic cases and industrial cases) have shown that, as expected, the iterative solver is always more efficient for the GCSIE formulation than for the two others. Solution is obtained after a small number of iterations (of order 10). In the majority of studied cases, this number of iterations does not depend of the values of the frequency and of the mesh size. Moreover it is independent of the boundary condition imposed. Let us recall that when the GCSIE formulation is used, no preconditioning matrix is needed. Solutions obtained from the GCSIE are accurate. But we have still noted that the EFIE formulation always has better accuracy.

References

[1] J. Gay, A. Bendali and M'B. Fares, A boundary-element solution of the leontovitch problem, IEEE Trans. Antennas Propagation, Octobre 1999.

[2] F. Alouges, S. Borel and D. Levadoux, A stable well conditioned integral equation for electromagnetism scattering, JCAM, 204(2) (2007).

[3] F. P. Andriulli, Well-Posed Boundary Element Formulations in Electromagnetics, PhD, University of Michigan, 2008.

[4] K. Bagci, H. Olyslager, F. Buffa, A. Christiansen, S. Michielssen, E. Andriulli and F. P. Cools, A multiplicative calderon preconditioner for the electric field integral equation, IEEE Trans. Antennas Propag., 56(8) (2008).

[5] A. Bendali, Boundary element solution of scattering problems relative to a generalized impedance boundary condition, in W. Jäger, J. Ne**v**cas, O. John, K. Najzar and J. Stará, editors, Partial Differential Equations, Theory and Numerical Solution, volume 406, pages 10–24. Chapman & Hall/CRC, 1999.

[6] O. P. Bruno, Computational electromagnetics and acoustics: high-order solvers, highfrequency configurations, high-order surface representations, Oberwolfach Reports, 5 (2007).

[7] Oscar Bruno, Tim Elling, Randy Paffenroth and Catalin Turc, Electromagnetic integral equations requiring small numbers of krylov-subspace iterations, J. Comput. Phys., 228(17) (2009).

[8] A. Buffa and R. Hipmair, Galerkin boundary element methods for electromagnetic scattering, dans topics in computational wave propagation and inverse problems, M. Ainsworth et al., eds., Springer-Verlag, Vol. 31, 2003.

[9] Annalisa Buffa and Snorre H. Christiansen, A dual finite element complex on the barycentric refinement, Math. Comput., 76 (2007).

[10] B. Carpentieri, Sparse Preconditioners for Dense Complex Linear Systems in Electromagnetic Applications, Ph.D. dissertation, INPT, April 2002, TH/PA/02/48.

[11] B. Carpentieri, I. S. Duff and L. Giraud, Sparse pattern selection strategies for robust frobenius-norm minimization preconditioners in electromagnetism, Numer. Linear Algebra Appl., 7(7-8) (2000), 667–685.

[12] P. G. Ciarlet, The Finite Element Method for Elliptic Problems, Series Studies in Mathematics and its Applications, North-Holland, Amsterdam, 1978.

[13] F. Collino and B. Despres, Integral equations via saddle point problems for time-harmonic maxwell's, J. Comput. Appl. Math., 150 (2003), 157–192.

[14] F. Collino, F. Millot and S. Pernet, Boundary-integral methods for iterative solution of scattering problems with variable impedance surface condition, Progress In Electromagnetics Research, PIER 80, 2008.

[15] D. Colton and P. Kreiss, Integral Equation Methods in Scattering, Wiley & Sons, New York, 1983.

[16] F. Millot, D. Levadoux and S. Pernet, New trends in the preconditioning of integral equations of electromagnetism, in Mathematics in Industry-Scientific Computing in Electical Engineering, Springer, 2010.

[17] M. Darbas, Péconditionneurs Analytiques de Type Calderon pour les Formulations Intégrales des Problèmes de Diffraction D'ondes, PhD Thesis INSA Toulouse, 2004.

[18] M. Darbas, Generalized cfie for the iterative solution of 3-d maxwell equations, Appl. Math. Lett., 19(8) (2006).

[19] D. Colton, F. Cakoni and P. Monk, The electromagnetic inverse-scattering problem for par-

tially coated lipschitz domains, Proc. Royal. Soc. Edinburgh, 134A (2004), 661–682.
[20] V. Frayssé, L. Giraud and S. Gratton, A set of GMRES routines for real and complex arithmetics, Technical report, Cerfacs TR/PA/97/49, Toulouse, France, 1997.
[21] V. Lange, Equations Intégrales Espace-Temps pour les équations de Maxwell, Calcul du Champ Diffracté par un Obstacle Dissipatif, PhD Thesis Université de Bordeaux I, 1995.
[22] M. A. Leontovich, Approximate boundary condition for electromagnetic field on the surface of good conductor, Investigations on Radiowave Propagation part II Moscow, Academy of Sciences, Octobre 1978.
[23] D. Levadoux, Etude d'une équation Intégrale Adaptée à la Résolution Haute Fréquence de L'équation de Helmholtz, PhD Thesis Paris VI, 2001.
[24] D. Levadoux and B. L. Michielsen, Analysis of a boundary integral equation for high frequency helmholtz problems, in Proceedings of 4th International Conference on Mathematical and Numerical Aspects of Wave Propagation, Golden, Colorado, pages 765–767, 1998.
[25] D. Levadoux and B. L. Michielsen, Nouvelles formuations intégrales pour les problèmes de diffraction d'ondes, Math. Model. Num. Anal., 38(1) (2004).
[26] L. N. Medgyesi-Mitschang and J. M. Putnam, Integral equation formulations for imperfectly conducting scatterers, IEEE Trans. Antennas Propag., 33(2) (1985).
[27] F. A. Milinazzo, C. A. Zala, and G. H. Brooke, Rational square-root approximations for parabolic equation algorithms, J. Acoust. Soc. Am., 101(2) (1997).
[28] P. Monk, Finite Element Methods for Maxwell's Equations, Clarendon Press, Oxford, 2003.
[29] S. P. Kiminki, P. Yla-Oijala and S. Jarvenpaa, Solving ibc-cfie with dual basis functions, IEEE Trans. Antennas Propag., 58(12) (2010).
[30] S. Pernet, A well-conditioned integral equation for iterative solution of scattering problems with a variable leontovitch boundary condition, Math. Model. Numer. Anal., 44(4), July 2010.
[31] D. Levadoux, S. Borel and F. Alouges, A new well-conditioned integral formulation for maxwell equations in three-dimensions, IEEE Trans. Antennas Propag., 53(9) (2005).
[32] C. T. Kelley, S. L. Campbell, I. C. F. Ipsen and C. D. Meyer, Gmres and the minimal polynomial, BIT Numerical Mathematics, Springer Netherlands, 36 (4), December 1996.
[33] C. T. Kelley, C. D. Meyer, S. L. Campbell, I. C. F. Ipsen and Z. Q. Xue, Convergence estimates for solution of integral equations with gmres, Tech. Report CRSC-TR95-13, North Carolina State University, Center for Research in Scientific Computation, March 1995.